消化器の臨床

Clinics in Gastroenterology

別　　刷

● Vol. 8 No. 2 2005　(2005年4・5月号) ●

ヴァン メディカル

特集・C型肝炎の最新治療―治療方針のたて方と治療効果―

肝硬変・肝細胞癌への進行を防ぐために

慢性C型肝疾患患者のフォローアップ戦略

松崎靖司[1)]・千葉俊也[2)]・斎藤吉史[3)]・佐藤巳喜夫[4)]・西　雅明[5)]

Summary

肝細胞癌（HCC）発癌抑制目的に，C型慢性肝炎の患者をできる限りの治療により（インターフェロン（IFN），ウルソデオキシコール酸（UDCA）など），肝硬変に移行しないように努力することがまず必要である。この経過観察には，血小板数，血中IV型コラーゲン値，年齢の高齢化などが重要な観察項目である。生活指導としては，飲酒者には禁酒をさせることである。HBV抗体（HBs抗体，HBc抗体）陽性のC型肝硬変患者においては，特に肝癌の発生に十分注意をすることが必要である。大量喫煙者には禁煙を，飲酒者には禁酒をさせる。さらに毎月肝機能，血小板などのチェックを行い，3～6ヵ月ごとの腹部超音波検査，2～3ヵ月ごとにAFP，PIVKA-IIなどの腫瘍マーカー検査を施行し，より綿密に観察することでHCC早期発見に努めることが重要である。

Key Words　HBV抗体／血小板数／IV型コラーゲン値／腫瘍マーカー／腹部超音波検査（US）

はじめに

近年，本邦においては肝細胞癌（HCC）患者の発生が増加している。年間発生率は最近は2万例を越している。その発生原因の一つであるB型肝炎ウイルス（HBV）による発癌機構の研究は数多くなされてきた。しかし近年，HBs抗原陰性（HBsAg（－））のC型肝炎ウイルス（HCV）抗体陽性HCC患者の発生が70～80％と増加している。

現在日本の人口1億2000万人のうち，HBVキャリアー率は約1.7％，HCVキャリアー率は約1.2％である。年間約2万人のHCC患者発生しているとされ，そのうちHCV抗体陽性者が70％としHBV陽性者を20％とした場合，HCV陽性者のHCC発生率はHBV陽性者の約5倍近くとなる換算で

1）筑波大学大学院人間総合科学研究科臨床医学系消化器内科助教授（まつざき　やすし）
2）牛久愛和総合病院消化器内科部長（ちば　としや）
3）筑波メディカルセンター病院消化器内科科長（さいとう　よしふみ）
4）竜ヶ崎済生会病院消化器内科科長（さとう　みきお）
5）茨城県立中央病院内視鏡部長（にし　まさあき）

ある。

原発性肝細胞癌による死亡者数は世界中で年間100万人に及ぶと推測され，未治療の場合，平均生存期間は数ヵ月といわれている。本邦における肝細胞癌患者は，2003年の国民衛生の動向によれば，癌による死亡の中で男性では3位，女性では4位の位置を占め，年々その数は増加しており，その予防，診断，そして治療法の改善は臨床的に非常に重要な意義を持つ。

そのHCCの発生原因の一つとしてHBs抗原陰性HCV抗体陽性HCC患者の発生が特に増加してきている。HCV陽性キャリアーの患者は，全国で200万人ともいわれている。またHCV抗体陽性者の自然経過は，HCV暴露から高率に慢性化し，20～30年後に肝硬変（LC），そしてHCC発癌へと移行することが明らかとなってきた。

以上のような現況から，HBV，HCV，アルコールあるいはその他の発癌因子のHCC発生への関与の解明は急務となってきているといっても過言ではない。C型慢性肝炎から不幸にも肝硬変になった患者の場合は肝癌の早期発見をし，早期治療することが重要課題である。いかに，慢性C型肝炎，肝硬変の患者を綿密に経過観察するかが問われている。

本邦における第16回全国原発性肝癌追跡調査報告によると肝癌における治療に関しては，原発性HCCの手術施行率は31.3%，外科手術以外の治療法の状況は，PEI41.2%，MCT17.7%，RFA40.2%，TAE26.5%（リピオドールのみ，塞栓物質のみの合計），TACE72.7%であり，RFA，TACE，PEIが主流を占める。放射線照射療法はわずか1.5%である[1]。肝予備能，腫瘍進展度など，肝細胞癌に対する主治療の選択に重要な関連がある。

これらの治療は早期発見のもとに行われるものであり，いかに慢性肝炎，肝硬変の患者を綿密に経過観察するかということが，重要な課題となる。我々の施設におけるHCC経過観察成績より，慢性C型肝疾患患者のフォローアップの方法として肝癌のハイリスク群の絞り込み方法，本施設における慢性肝疾患患者のフォローアップ戦略法について述べる。

HCV抗体陽性慢性肝疾患患者におけるHCC発生危険因子の予測

HBVの感染の既往と大量喫煙について —occult HBVと喫煙—

不幸にして肝硬変になってしまった場合，肝癌が発生する確立が高くなる。肝癌のフォローアップに関しては，まずは肝硬変からの癌発生の危険因子を疫学的に検討し危険因子を探ること，さらに早期発見，早期治療に努めることが重要である。そこで，肝癌発生の危険因子を疫学的に検討し，危険因子を探り，早期発見に努める必要がある。我々はまず，HBs抗原陰性，かつHCV抗体陽性（C（+））LCにおける発癌因子の疫学的検討の一つとして，まずHBV関連抗体の関与の可能性を見出した。つまりHCVとHBVのHCC発癌における役割を解明する目的で，HBsAg（−）HCCの合併LC例と非合併LCにおけるHCV抗体とHBV抗体の陽性率の検討を行った（**表1**）。HBsAg（−）HCCの合併LC例のHBs抗体陽性かつあるいはHBc抗体陽性率は85.4%で，HCC非合併LC例の43.2%に比し有意に高率であった。つまりHBsAg（−）LC例の場合，HBVの既往感染がHCC発癌の危険因子として重要である可能性が示唆されることを確認した[2]。

表1 C型肝炎におけるB型肝炎ウイルスマーカー

	HBs抗体陽性	HBc抗体陽性	HBs抗体陽性 and/or HBc抗体陽性
肝癌合併肝硬変 (N=48)	25* (52.1%)	38** (79.2%)	41** (85.4%)
肝癌非合併肝硬変 (N=44)	9* (20.5%)	18** (40.9%)	19** (43.2%)

*$p<0.005$, **$p<0.001$ (文献2)より改変)

そこで次に，prospective studyとしてHCV抗体陽性慢性肝疾患（慢性肝炎，肝硬変）412例の患者において，Cox比例ハザードモデルによる解析を行った。その結果，表2に示すように肝硬変は慢性肝炎に比し5.14倍の危険率で，HBs抗体陽性かつあるいはHBc抗体陽性例において陰性例に比し2.14倍の危険率，大量喫煙者（Smoking index≧400）は非喫煙者に比し2.46倍の危険率で有意にHCCの発現が高率に認められることが明らかとなった。つまり，C型慢性肝疾患患者においてHBV関連抗体陽性例，肝硬変であること，大量喫煙者がHCCの発生の危険性が高いことが示唆された[3]。つまり，C型慢性肝疾患患者においてHBV関連抗体陽性例がHCCの発生の危険性が高いことが明らかとなったわけである。このような成績は他のグループなども慢性肝疾患患者においてのHCC発癌危険因子として同様な結果を報告している[4~11]。

近年，HBs抗体陽性かつあるいはHBc抗体陽性例において有意にHCC発生例が多いということは，以下の理由が推測される。いわゆるoccult HBVと言われるものである[12,13]。一般的にはHBV持続感染の可能性が低いと考えられるHBsAg（−）HCV（+）HCCにおいても，我々の検討を含めた分子生物学的手法を用いた検討によって，

表2 C型慢性肝疾患412例（慢性肝炎232例，肝硬変180例）における肝癌発生危険因子—Cox比例ハザードモデルによる解析—

（筑波大学消化器内科1977.3〜1993.6）

Variable	Abjusted Rate Ratio	95% CI	x^2
Stage of disease			
Liver cirrhosis	5.14	2.52〜10.46	0.0001
Chronic hepatitis	1.00		
Anti-HBs and/or Anti-HBc			
Positive	2.14	1.13〜 4.07	0.02
Negative	1.00		
Smoking			
Smoking index* ≧400	2.46	1.11〜 5.49	0.03
Smoking index<400	1.67	0.75〜 3.73	0.21
Nonsmoking	1.00		

*Smoking index：averrage of cigarettes per day multiplide by total years of smoking.

（文献3）より一部改変）

少なからずHBVの持続感染が成立していることが明らかとなってきた。つまりHBsAg(−)HCCにおいてもHBVがHCC発生に関与している可能性が示唆されるというわけである。近年以上のような成績より，HCV抗体陽性，HBs抗原陰性肝細胞癌（HBsAg(−)HCV(+)HCC）において，HBVの関与の可能性について検討がなされるようになってきた。

HBVの持続感染により高率にHCCが発生することは，上述のごとく疫学的にも明らかである。さらに1980年以降の分子生物学的検討より，HBV DNAの宿主ゲノムへの組み込みが証明された。**表3**のごとくHBsAg陽性HCCの多くの例では，HBV DNAの組み込み，非癌部への組み込みをも認める。組み込み部位はランダムであるという特徴がある[14~16]。以上より，現在HBVの関与する肝発癌機序としては，HBV DNAの組み込みにより，遺伝子産物によるトランス活性化，癌抑制遺伝子の不活化，組み込みによる染色体不安定性などが多段階に関与していると考えられるようになってきた。

我々の検討を含め，HBsAg(−)HCCの大部分の肝組織中にHCV RNAの存在が認められた。つまりこれまでの疫学的な検討に示されているように，HBsAg(−)HCCにおいてHCVとHCC発生との間に強い関連が示唆された。しかし腫瘍部と非腫瘍部との間に，HCVの存在・増殖の頻度に差が見られなかったことから，HCVによる直接的な発癌への関与は説明し難い。今回の症例の非癌部病変は全例LCであることより，HCVの発癌への関与はLCを通しての役割が大きいことが推測される。この点に関しては今後の検討を重ねなければならない。

以上よりHBsAg(−)HCV(+)HCCに，過去のB型肝炎の感染が肝細胞内で持続している可能性もあり，肝癌発癌にHBVが関与している可能性が示唆されるのである。一概にこの事象で発癌を説明できないが，今後の重要な検討課題の一つとなっている。

C型慢性肝疾患患者においてHBV関連抗体陽性例，肝硬変であること，大量喫煙者が非喫煙者に比べHCCの発生の危険性が高いことが明らかとなった。しかし，大量喫煙と肝細胞癌発癌に関してはいくつかの同じ報告がなされている。たばこの成分の解毒，代謝に肝臓内でのcytochrome P450が関与していることは明らかであり，なんらかの関連があることが示唆される。しかし，いまだ過剰喫煙と肝細胞癌発癌機序に関する明確な実証はない。この点の詳細も今後の検討課題である。

表3　HBV DNA各サイトごとの腫瘍部／非腫瘍部組織への組み込みのPCR法（遺伝子増幅法）による検出

	HBV DNA			
	X gene	Pre-C gene	S gene	P gene
	No. (%)			
Tumourous tissue (n=16)	3(18.8)	4(25.0)	5(31.3)	3(18.8)
Nontumourous tissue (n=16)	3(18.8)	6(37.5)	3(18.8)	0
Coexsistence	3(18.8)	2(12.5)	2(12.5)	0

アルコール飲酒と発癌の関係

大酒家においてはウイルス感染がHCC発癌に重要な役割をしていることが明らかとなっている。HCV感染において，飲酒は肝組織像や，臨床症状の進行に重要な危険因子であることも言われている。大酒家肝硬変の患者が，長期に大量飲酒をすると，cytochrome P450 2E1（CYP2E1）が誘導されることが明らかとなっている[17]。CYP2E1は，N-nitrosodimethylamine（NMDA）を代謝し発癌物質とする食物に含まれるものである。動物実験ではあるが，アルコールとNMDAの両者投与で前癌病変ができることが証明されている[18]。肝細胞癌とアルコール飲酒との発癌の関係は多くの論文がある[19,20]。HBs抗原陰性（NB），HCV抗体陰性（NC）のアルコール性肝硬変においてHCC発生が関係あるとの報告もある[21]。大量飲酒者のHCC発癌において，HBV，HCVが関与するという報告もあり[22~28]，いまだ一定した見解は得られていないが，今後のさらなる検討が必要である。

また我々は，飲酒に関しては，時点における発癌因子の多重解析によると，大量飲酒者は非飲酒者に比べ有意な危険因子としてあがることを報告した[29]。おそらく大量飲酒は，慢性肝炎から肝硬変になるスピードが早くなる可能性が考えられる。さらに肝癌の発生因子になる危険性が高いので禁酒の指導をする必要があろう。

腹部超音波検査の徹底

一般に，腫瘍体積は指数関数的に増大し，その増加速度は一定であるとされている。この理論を用いて，**図1**に示すごとくHCCにおいて画像より求めた仮想腫瘍体積より腫瘍倍加時間（TVDT）を求めることが検討されてきた[30~35]。さらにTVDTと予後との関連性を検討した報告が散見されている[32,33,35]。

また，腹部超音波検査（US）は患者に対し非侵襲的であるため反復して検査しやすく，

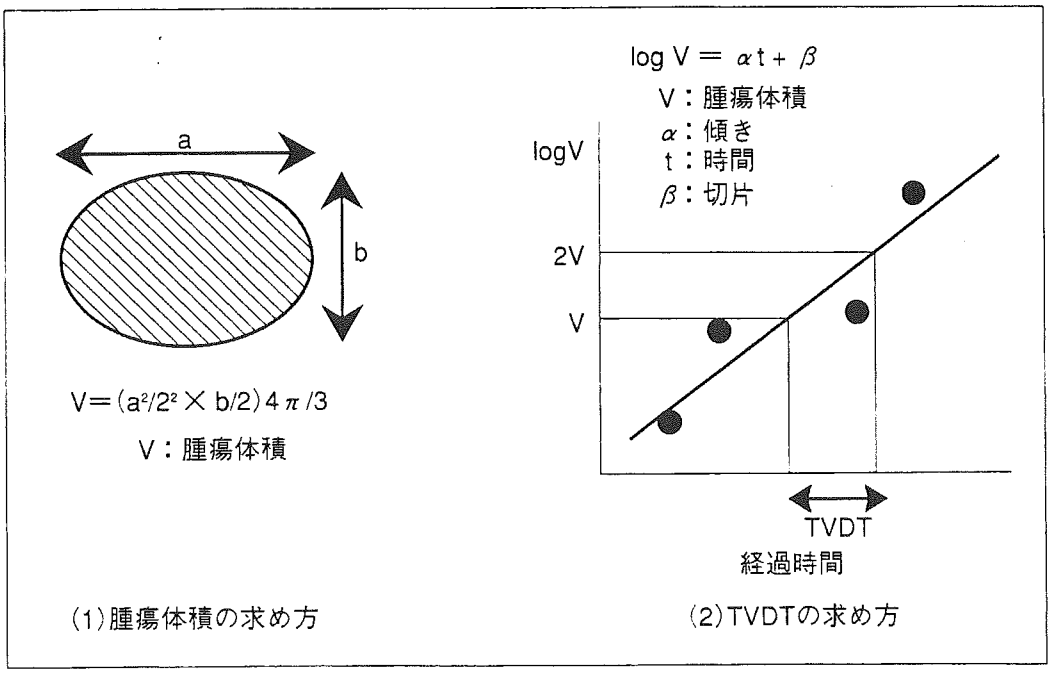

図1　腫瘍体積およびTVDTの求め方

かつ肝内の小腫瘤の描出に優れている。近年US診断装置の発達，普及および慢性肝疾患患者のフォローアップの徹底によって，径10～20mm程度のいわゆる小HCCが多く発見されるようになった。現在本邦においてHCCはUSで発見されることが最も多くHCC診断・治療における重要な地位を占めるようになった。しかしUS像の違い，あるいはその経時的変化からみた，HCCの増大速度などの特性については一定の見解がいまだない。このため，経時的なUS所見の変化をはじめとする，USからみたHCCの特性を知ることは重要であると考えられる。

我々はTVDTの予後におよぼす影響についての検討を行った。Cox比例ハザードモデルを用いた検討結果を**表4**に示した。70歳未満であること（P＝0.015，ハザード比0.094），Child-Pugh分類がgrade Aであること（P＝0.035，ハザード比0.218），TVDTが3ヵ月未満であること（P＝0.003，ハザード比52.670）が有意な因子であり，治療の有無（P＝0.452，ハザード比0.465）は統計学的に有意ではなかった。

HCCの腫瘍発育速度について，一定のものとして取り扱ってよいのか，また発育過程において変化していくものとすべきなのか議論の別れるところである。HCCの発育にしたがいその時点における増殖能の違う腫瘍構成成分の比率によって，腫瘍発育速度が変化すると考えた方が自然であると考えられる。しかしUSを用いて腫瘍径を測定する場合，検者や操作角度の違いによりかなり誤差を含んでしまう可能性を考慮しなくてはならず，数mmの腫瘍径変化を有意とするか否かについて苦慮するところである。さらに，HCCにおいてはその組織学的進展形態より，単結節型，単結節周囲増殖型，多結節融合型，多結節型，塊状型と分類され多様であるため，USによって正確に病変の境界を把握することは困難であることがある。また，背景に進行した肝硬変を有していると肝内エコーが不整となり腫瘍を明瞭に検出しづらくなる。これらの点も誤差を生じる要因であると考える。

表4　比例ハザードモデル

検討因子		ハザード比	P値
年齢	70歳未満	0.094	0.015
Child分類	A	0.218	0.035
TVDT	3ヵ月未満	52.670	0.003
治療の有無	無治療	0.465	0.452

小HCCのUS patternについての検討は数多く報告されており[34~37]，特にhyperechoic patternを呈するHCCの病理学的および臨床的意義の検討が多くされている。慢性肝疾患患者のフォローアップ中にUSで発見される3cm以下のHCCの約40％がhyperechoic patternを呈し[36]，組織学的に脂肪変性あるいは腫瘍細胞の淡明細胞化を伴っていることが多く，高分化型であることが多いとされている[38]。さらに前癌病変とされているdysplastic noduleであることも少なくなく，いずれの場合もその腫瘍発育速度は比較的ゆっくりしたものであるとされている。この点については，綿密な組織学的検討を加える必要があると考えられるが，dysplastic noduleの厳重なフォローアップ中，TVDTを慎重に計測することは，癌化の時期を知る方法として有用である可能性がある。

我々はHCC患者においてTVDTと生存期間の間に有意な相関があることを明らかにした。Ebaraら[31]は，無治療の直径3cm未満の小HCC患者において，TVDT，年齢，腫瘍径，肝硬変の重症度が有意な予後因子であったとしている。

TVDTをrapid growth群，intermediate growth群，slow growth群に分類すると，

rapid growth群の予後が不良であるとの報告[35]から，我々もTVDT 3ヵ月未満をrapid growth群とし，予後との関連を検討した。自験例において3年生存率は58%で，江原ら[39]によって，無治療で観察されたHCC例の3年生存率0%より明らかに良好であった。治療の有無および方法が統一されていない検討においても，TVDT 3ヵ月未満のHCC例は予後が悪いことが示唆された。以上より，TVDT 3ヵ月未満のrapid growth群HCCに対しては，治療計画を立てるにあたり十分な注意が必要であると考えられた。

我々を含めた検討より，肝癌の予後との関連を検討するとTVDT（5ヵ月で区切る）が短い群の予後が有意に悪いという結果を得ている。つまり，USは3～6ヵ月ごとに肝硬変患者には行った方がよいということになる。以上のことから，我々の施設ではこれらの危険因子を考慮し，多中心性発癌を考えて治療方針を考え，経過観察に十分注意を払うこととしている。

血液マーカーのチェック

Ikedaらは，HCC発癌率を高める独立要因を多変量解析を行った[40]。Cox比例ハザードモデルにおいて，HCV陽性肝硬変である，血小板数が10万/mm²未満，男性で，AFP値が20ng/mL以上，年齢が55歳以上，ICG15分値が30%以上の場合，有意にHCC発癌危険率が高くなることを報告している。第16回全国原発性肝癌追跡調査報告によると，HCV抗体陽性は，HCC18,216例中，71.8%であり，HBs抗原陽性は，17,959例中，5.5%と，圧倒的にHCV陽性者が多いことがわかる。また，HCC治療前の，血小板数は10万/mm²未満は40.4%であった。AFP値は65.5%に増加を認め，その中でレクチン分画であるL3分画は，AFP上昇者の36%で増加を認めている。また，HCCに特異的な腫瘍マーカーである，PIVKA-IIはAFPとほぼ同様で61.6%に増加を認めている。

また，近年はインターフェロン（IFN）により中等度までの線維化は著効，有効となれば，改善することも明らかとなってきた。我々は，肝線維化を想定するマーカーとして，血中IV型コラーゲン値（EIA法，ラテックス法による測定）が線維化の程度と相関し，IFN治療により改善することを明らかにした[41,42]。線維化の進行，治療による改善を見る上で，有用なマーカーの一つとなると考えられる。

以上より，肝炎から肝硬変への進行を観察するには，血小板数，血中IV型コラーゲン値，年齢の高齢化などが重要な観察マーカーとなると考える。さらにHCC発癌に関しては，年齢の高齢化，血小板数の推移，AFP，PIVKA-IIなどの腫瘍マーカーなどの推移を観察することが，肝癌早期発見のための重要な経過観察指標となると考えられる。

総　括

慢性C型肝疾患患者においては，HCCの発生に十分注意をすることがまず肝要である。肝機能の変動のある慢性肝炎の患者においては，肝硬変への移行を注意深く観察する。飲酒者には禁酒をさせること。血小板数，血中IV型コラーゲン値，年齢の高齢化などが重要な観察項目である。特にHBV抗体（HBs抗体，HBc抗体）陽性者で，C型肝硬変患者のフォローアップにおいては，大量喫煙者には禁煙を，飲酒者には禁酒をさせる。そしてなによりも重要なことは毎月肝機能，血小板などのチェックを行い，3～6ヵ月ご

との腹部超音波検査，2～3ヵ月ごとにAFP，PIVKA-IIなどの腫瘍マーカー検査を施行し，より綿密に観察することでHCC早期発見に努めることである。無症候性キャリアーの場合や，IFN著効例においても発癌例があるので，年1～2回は検査をうけるように指導をすることが重要であることを最後に付け加える。

文　献

1) 日本肝癌研究会：第16回原発性肝癌追跡調査報告（1996～1997）：（2004）
2) Tanaka N, Chiba T, Matsuzaki Y *et al*：High prevalence of hepatitis B and C viral markers in Japanese patients with hepatocellular carcinoma. J Gastroenterol **28**：547-553（1993）
3) Chiba T, Matsuzaki Y, Abei M *et al*：The role of previous hepatitis B virus infection and heavy smoking in hepatitis C virus-related hepatocellular carcinoma. Am J Gastroenterol **91**：1195-1203（1996）
4) Paterlini P, Driss F, Nalpas B *et al*：Persistence of hepatitis B and hepatitis C viral genomes in primary liver cancers from HBsAg-negative patients：a study of a low-endemic area. Hepatology **17**：20-29（1993）
5) Sheu JC, Huang GT, Shih LN *et al*：Hepatitis C and B virus in hepatitis B surface antigen-negative hepatocellular carcinoma. Gastroenterology **103**：1322-1327（1992）
6) Yu MC, Tong AJ, Cousaget P *et al*：Prevalence of hepatitis B and C viral markers in black and white patients with hepatocellular carcinoma in the United States. J Natl Cancer Inst **82**：1038-1041（1990）
7) Ruiz J, Sangro B, Cuende JI *et al*：Hepatitis B and C viral infections in patients with hepatocellular carcinoma. Hepatology **16**：637-641（1992）
8) Villa E, Grottola A, Buttafoco P *et al*：Evidence for hepatitis B virus infection in patients with chronic hepatitis C with and without serological markers of hepatitis B. Dig Dis Sci **40**：8-13（1995）
9) Fabris P, Brown D, Tositti G *et al*：Occult hepatitis B virus infection does not affect liver histology or response to therapy with interferon alpha and ribavirin in intravenous drug users with chronic hepatitis C. J Clin Virol **29**：160-166（2004）
10) Torbenson M, Thomas DL：Occult hepatitis B. Lancet Infect Dis **2**：479-486（2002）
11) Benvegnu L, Fattovich G, Noventa F *et al*：Concurrent hepatitis B and C virus infection and risk of hepatocellular carcinoma in cirrhosis. Cancer **74**：2442-2448（1994）
12) Brechot C, Thires V, Kremsdorf D *et al*：Persistent hepatitis B virus infection in subjects without hepatitis B surface antigen：Clinically significant or purely Occlut. Hepatology **34**：194-203（2001）
13) Hu K：Occult hepatitis B virus infection and its clinical implications. J Viral Hepatitis **9**：243-257（2002）
14) Chang MH, Chen PJ, Chen JY *et al*：Hepatitis B virus integration in hepatitis B virus-related hepatocellular carcinoma in childhood. Hepatology **13**：316-320（1991）
15) Koike K, Nakamura Y, Kobayashi M *et al*：Hepatitis B virus DNA integration frequency observed in the hepatocellular carcinoma DNA of hepatitis C virus-infected patients. Int J Oncol **8**：781-784（1996）
16) Matsuzaki Y, Chiba T, Hadama *et al*：HBV genome integration and genetic instability in HBsAg-negative and anti-HCV-positive hepatocellular carcinoma in Japan. Cancer Letters **119**(1)：53-61（1997）
17) Miyakawa H, Sato C：Alcohol and hepatocellular carcinoma. Clin Gastroenterol **10**：1279-1286 [in Japanese]（1995）
18) Tsutsumi M, Matsuda Y , Takada A：Role of ethanol-inducible cytochrome P450 2E1 in the development of hepatocellular carcinoma by the chemical carcinogen , *N*-nitrosodimethylamine. Hepatology **18**：1483-1489（1993）
19) Tsutusmi M, Ishizakki M, Takada A：Relative risk for the development of hepatocellular carcinoma in alcoholic patients with cirrhosis：a multiple logistic-regression coefficient analysis. Alcohol Clin Exp Res **20**：758-762（1996）
20) Tsukuma H, Hiyama T, Yamazaki H *et al*：Risk factors for hepatocellular carcinoma among patients with chronic liver disease. N Engl J Med **328**：1797-1801（1993）
21) Uetake S, Yamauchi M, Itoh S *et al*：Analysis of risk factors for hepatocellular carcinoma in patients with HBs antigen- and anti-HCV antibody-negative alcoholic cirrhosis：

clinical significance of prior hepatitis B virus infection. Alcohol Clin Exp Res **27**：47S-51S (2003)
22) Matsuda Y, Amuro Y, Nakano T *et al*：Relation between markers for viral hepatitis and clinical features of Japanese patients with hepatocellular carcinoma：possible role of alcohol in promoting carcinogenesis. Hepato-Gastroenterology **42**：151-154 (1995)
23) Paglialo L, Simonetti RG, Craxi A *et al*：Alcohol and HBV infection as risk factors for hepatocellular carcinoma in Italy：a multicentric, controlled study. Hepato-Gastroenterology **30**：48-50 (1983)
24) Villa E, Baldini GM, Pasquinelli C *et al*：Risk factors for hepatocellular carcinoma in Italy. Male sex, hepatitis B virus, non-A, non-B infection, and alcohol. Cancer **62**：611-615 (1988)
25) Ohnishi K, Iida S, Iwana S *et al*：The effect of chronic alcohol intake on the development of liver cirrhosis and hepatocellular carcinoma：relation to hepatitis B surface antigen carriage. Cancer **49**：672-677 (1982)
26) Horie Y,Yamagishi Y, Kajihara M *et al*：Effect of alcohol consumption on the progression of hepatitis C virus infection and risk of hepatocellular carcinoma in Japanese patients. Alcohol Clin Exp Res **27**：32S-36S (2003)
27) Yamauchi M, Nakahara M, Maezawa Y *et al*：Prevalence of hepatocellular carcinoma in patients with alcoholic cirrhosis and prior exposure to hepatitis C. Am J Gastroenterol **88**：39-43 (1993)
28) Takase S, Tsutsumi M, Kawahara H *et al*：The alcohol-altered liver membrane antibody and hepatitis C virus infection in the progression of alcoholic liver disease. Hepatology **17**：9-13 (1993)
29) Chiba T, Matsuzaki Y, Abei M *et al*：Multivariate analysis of risk factors for hepatocellular carcinoma in patients with hepatitis C virus-related liver cirrhosis. J Gastroenterol **31**：552-558 (1996)
30) Ebara M, Ohto M, Shinagawa T：Natural history of minute hepatocellular carcinoma smaller than three centimeters complicating cirrhosis. Gastroenterology **90**：289-298 (1986)
31) Ebara M, Hatano R, Fukuda H *et al*：Natural course of small hepatocellular carcinoma with underlying cirrhosis. A study of 30 patients. Hepato-Gastroenterology **45**(13)：1214-1220 (1998)
32) Okada S, Okazaki N, Nose H：Follw-up examination schedule of postoperative HCC patients based on tumor volume doubling time. Hepato-Gastroenterology **40**：311-315 (1993)
33) Okazaki N, Yoshino M, Yoshida T：Evaluation of the prognosis for small hepatocellular carcinoma based on tumor volume doubling time. Cancer **63**：2207-2210 (1989)
34) Sheu JC, Sung JL, Chen DS：Growth rate of asymptomatic hepatocellular carcinoma and its clinical implications. Gastroenterology **89**：259-266 (1985)
35) 真島康雄：超音波断層法による肝細胞癌の発育速度とその臨床的意義．肝臓 **25**(6)：754-765 (1984)
36) 貫野 徹，岡 博子，金 鎬俊：小肝細胞癌における高エコー域の予後因子としての意義．日消誌 **89**(1)：55-60 (1992)
37) 安田 宏，藤野 均，宇多慶記：慢性肝疾患に出現した血管種様高エコー結節の超音波による経過観察例の検討．肝臓 **31**(7)：749-752 (1990)
38) 小野直美，孫 順徳，池田 敏：2cm以下の肝内高エコー病変の鑑別診断とその自然経過の検討—肝癌の早期診断を目的として—．Jpn J Med Ultrasonics **19**(10)：676-684 (1992)
39) 江原正明，大藤正雄，品川 孝：長期無治療の小肝細胞癌22例における臨床所見の検討．日消誌 **81**(8)：1799-1809 (1984)
40) Ikeda K, Saitoh S, Koide I *et al*：A multivariate analysis of risk factors for hepatocellular carcinogenesis：A prospective observation of 795 patients with viral and alcoholic cirrhosis. Hepatology **18**：457-481 (1993)
41) Matsuzaki Y, Yoshiga S, Sugitani T *et al*：Enzyme immunoassay of serum Type IV collagen in anti-HCV positive chronic liver diseases. Clin Chim Acta **221**：209-217 (1993)
42) 西 雅明，松崎靖司，土井幹雄：C型慢性肝炎におけるインターフェロン（INF）治療効果と病理組的変化．特に線維化と血中IV型コラーゲンとの変化についてインターフェロン治療によりC型慢性肝炎の線維化改善はみられるか，中外医学社，東京（1996）p324-329

Available online at www.sciencedirect.com
SCIENCE DIRECT
Hepatology Research 34 (2006) 23–27
HEPATOLOGY RESEARCH
http://www.elsevier.com/locate/hepres

Erythrocyte ribavirin concentration for assessing hemoglobin reduction in interferon and ribavirin combination therapy

Yoichi Inoue [a], Masato Homma [a,*], Yasushi Matsuzaki [b], Minoru Shibata [c], Takuya Matsumura [c], Takayoshi Ito [c], Yukinao Kohda [a]

[a] *Department of Pharmaceutical Sciences, Graduate School of Comprehensive Human Sciences, University of Tsukuba, Tennodai 1-1-1, Tsukuba, Ibaraki 305-8575, Japan*
[b] *Department of Gastroenterology, Graduate School of Comprehensive Human Sciences, University of Tsukuba, Tennodai 1-1-1, Tsukuba, Ibaraki 305-8575, Japan*
[c] *Second Department of Internal Medicine, School of Medicine, Showa University, Hatanodai 1-5-8, Shinagawa, Tokyo 142-8666, Japan*

Received 16 September 2005; received in revised form 25 October 2005; accepted 26 October 2005
Available online 1 December 2005

Abstract

Background: Ribavirin-induced hemolytic anemia is one of the important adverse effects for the premature cessation of interferon and ribavirin combination therapy for hepatitis C virus clearance. To elucidate the mechanism of this matter, we examined the effects of plasma and erythrocyte ribavirin concentration on hemoglobin (Hb) reduction to assess hemolytic anemia in this combination therapy.
Method: Nineteen patients, treated with the interferon alpha-2b and ribavirin combination therapy, were included. Plasma and erythrocyte ribavirin concentrations were monitored for the first 28 days of the combination therapy, in relation to changes in hematological parameters, Hb and hematocrit values. The initial dose of ribavirin was 11.5 ± 1.5 mg/kg/day.
Results: Steady-state plasma and erythrocyte ribavirin concentrations were 8.9 ± 2.6 and 1218 ± 270 μM, respectively. Significant correlation was observed between erythrocyte ribavirin and Hb reduction ($r = 0.360$, $p < 0.05$), but not between plasma ribavirin and Hb reduction. The patients with higher levels of erythrocyte ribavirin (≥1000 μM) had greater Hb reduction compared to those with lower levels (<1000 μM) (3.8 ± 1.2 g/dL versus 2.6 ± 0.9 g/dL, $p < 0.05$). Nine cases out of 12 patients who developed anemia within the first 28 days of the combination therapy had higher levels of erythrocyte ribavirin (≥1000 μM).
Conclusion: We confirmed that erythrocyte ribavirin was strongly associated with Hb reduction in interferon and ribavirin combination therapy.

Keywords: Erythrocyte ribavirin; Anemia; Hepatitis C virus; Interferon

1. Introduction

Ribavirin co-administration with interferon alpha-2b including pegylated derivatives plays an important role in hepatitis C virus (HCV) clearance, leading to improvements in sustained viral response [1–4]. However, a substantial population of the patients receiving this combination therapy suffers from severe hemolytic anemia, which sometimes requires ribavirin dose reduction and cessation of the treatment [5–7].

Although the mechanism of ribavirin-induced anemia has remained unclear, it has been speculated that highly accumulated ribavirin in erythrocytes reduces erythrocyte life span [8–10]. Once incorporated into erythrocytes via the equilibrate nucleoside transporter 1 (ENT-1), ribavirin is converted into phosphorylated metabolites by intracellular phosphorylation [9,11,12]. Since the phosphorylated metabolites

* Corresponding author. Tel.: +81 29 853 3859; fax: +81 29 853 7025.
E-mail address: masatoh@md.tsukuba.ac.jp (M. Homma).

1386-6346/$ – see front matter © 2005 Elsevier Ireland Ltd. All rights reserved.
doi:10.1016/j.hepres.2005.10.003

are not substrates for ENT-1, they cannot be effluxed out of the erythrocytes and so accumulate internally. Phosphorylated ribavirin (mono- and tri-phosphates) is thought to exert antiviral effects on HCV in hepatocytes [13]. On the other hand, after entering erythrocytes it impairs erythrocyte integrity by reducing intracellular ATP levels, resulting in accelerated erythrophagocytosis in the reticuloendothelial system [8].

Thus, ribavirin disposition in erythrocytes may influence the occurrence of anemia in interferon and ribavirin combination therapy. We previously observed that marked elevation (around 1000 μM) of erythrocyte ribavirin including phosphorylated metabolites associated with hemoglobin (Hb) reduction in the combination therapy [14]. However, we could not assess the threshold of ribavirin concentration in blood (plasma and erythrocyte) leading severe Hb reduction, because of the limited number of patients. In the present study, we report the impact of blood ribavirin concentration, especially 1000 μM of erythrocyte ribavirin, on Hb and hematocrit (Ht) reduction in further conducted the therapeutic drug monitoring of ribavirin under the combination therapy.

2. Patients and methods

2.1. Patients

Nineteen patients with chronic hepatitis C under the interferon alpha-2b and ribavirin combination therapy were examined. The dosage regimen for interferon and ribavirin was observed in accordance with the standard dosing instructions set for Japanese HCV patients. Patients received 10 million IU of interferon alpha-2b daily for the first 2 weeks followed by 6 million IU three times weekly for 22 weeks. The initial dose of oral ribavirin was adjusted in accordance with their body weight, 600 mg/day for patients weighing less than 60 kg, and 800 mg/day for patients weighing over 60 kg. The mean initial dose of ribavirin was 11.5 ± 1.5 mg/kg/day. The patients' profile is indicated in Table 1.

Venous blood samples for determining blood ribavirin concentration were collected from the patients. Heparinized blood collection (10 mL) was done at 0, 1, 3, 7, 14, 21, and 28 days after starting the combination therapy. Hematological parameters, such as Hb, Ht, white blood cell and platelet counts, and biochemical parameters, such as HCV-RNA, aspartate aminotransferase and alanine aminotransferase (ALT), blood urea nitrogen, and serum creatinine were also measured on each sampling day. Anemia was defined as blood hemoglobin level less than 13.5 g/dL in male and less than 11.5 g/dL in female patients in this study. Informed consent was obtained from the patients and the study was approved by the ethical committee of our University.

Table 1
Patients' profile and response to interferon and ribavirin combination therapy

	Baseline	Day 28
Age (year)	49.1 ± 14.1	
Sex (M/F)	14/5	
Body weight (kg)	61.9 ± 11.4	
Ribavirin (mg/kg/day)	11.5 ± 1.5	11.2 ± 1.2
Hepatitis C virus RNA (kIU/mL)*	1963 ± 3409	24 ± 57
Sero group: 1/2/unknown	12/5/2	
White blood cell ($\times 10^3$ μL^{-1})*	5.2 ± 0.6	3.1 ± 1.3
Hemoglobin (g/dL)**	15.0 ± 1.5	11.4 ± 1.3
Hematocrit (%)**	44 ± 5	34 ± 4
Platelet ($\times 10^9$ L^{-1})	134 ± 29	118 ± 45
Aspartate aminotransferase (U/L)*	60 ± 27	35 ± 14
Alanine aminotransferase (U/L)**	94 ± 47	36 ± 18
Blood urea nitrogen (mg/dL)	15.8 ± 3.5	13.4 ± 1.6
Serum creatinine (mg/dL)	0.77 ± 0.16	0.69 ± 0.17
Ribavirin concentration (μM)		
Plasma		8.9 ± 2.6
Erythrocyte		1218 ± 270

Data are expressed as mean ± S.D. or number of patients.
* Significant difference was observed between baseline and day 28 at $p < 0.05$.
** Significant difference was observed between baseline and day 28 at $p < 0.0001$.

2.2. Quantification of blood ribavirin

Quantification of plasma and whole blood ribavirin concentration was carried out by high-performance liquid chromatography (HPLC) developed by us [10]. Briefly, a 20 μL of whole blood supplemented with a six-fold volume of ice-cold distilled water was subjected to acid phosphatase (2 units, Sigma–Aldrich Co., St. Louis, MO) digestion to convert phosphorylated metabolites into free ribavirin. The resulting mixture, spiked with an internal standard (3-methylcytidine methosulfate, Sigma–Aldrich Co.), was treated by phenyl boronic acid (PBA) column (Bond Elute PBA; Varian, Palo Alto, CA) extraction followed by reverse-phase HPLC analysis. The dephosphorylation step was omitted when unchanged ribavirin was determined in plasma and whole blood. Since phosphorylated ribavirin was undetectable in plasma [10], plasma samples were not treated with acid phosphatase. The concentration of erythrocyte ribavirin was calculated with the following formula:

$$C_{rbc} = \frac{[C_w - C_p(1 - Ht)]}{Ht},$$

where C_{rbc} is the erythrocyte ribavirin concentration; C_w the concentration in whole blood; C_p the concentration in plasma; and Ht is the hematocrit.

The HPLC apparatus used in this study was the model 8020 system (Tosoh Corp., Tokyo, Japan) equipped with a UV detector, an auto-sampler, and a pump. A C18 reverse-phase column (TSK-Gel ODS-80Ts, Tosoh Corp.) was used for separation of ribavirin from other contaminants. The detection wavelength was set at 225 nm. The mobile phase solvent, 10 mM ammonium phosphate buffer (pH 2.5), was pumped out at a flow rate of 1.0 mL/min. All chemicals for the assay

were of HPLC or regent grade (Wako Pure Chemicals Ind., Osaka, Japan or Sigma–Aldrich Co.).

2.3. Statistical analysis

Changes in Hb and ALT from the baseline after starting the combination therapy were analyzed by the Dunnett test. Correlation coefficients between ribavirin concentrations and hematological parameters were determined by linear regression analysis. Student's *t*-test was used to assess the difference in ribavirin concentrations and the reduction of hematological parameters between the two groups, patients with <1000 and ≥1000 μM of erythrocyte ribavirin concentration. A *p*-value less than 0.05 was considered to be significant.

3. Results

The change in ALT, Hb, plasma-, and erythrocyte ribavirin concentrations during the first 28 days of the combination therapy is shown in Fig. 1. ALT and Hb were gradually decreased and significant reductions were observed on days 7 and 14, respectively (Fig. 1). Steady-state plasma and erythrocyte ribavirin concentrations reached levels of 8.9 ± 2.6 and 1218 ± 270 μM, respectively, 28 days after starting the combination therapy (Table 1). Phosphorylated metabolites (1133 ± 234 μM) accounted for 93% of erythrocyte ribavirin, whereas the metabolites were not detected in plasma (data not shown). These concentrations observed in the present study agreed with our previous study of a small number of HCV patients [10,14]. The erythrocytes/plasma ratio of ribavirin concentration was gradually increased, reaching a plateau of 149 ± 45 within 2 weeks (data not shown). Hb levels decreased correspondingly with the raise of ribavirin concentrations, and bottomed out at around day 28. We confirmed that ribavirin concentrations and Hb did not change significantly after day 28 (data not shown).

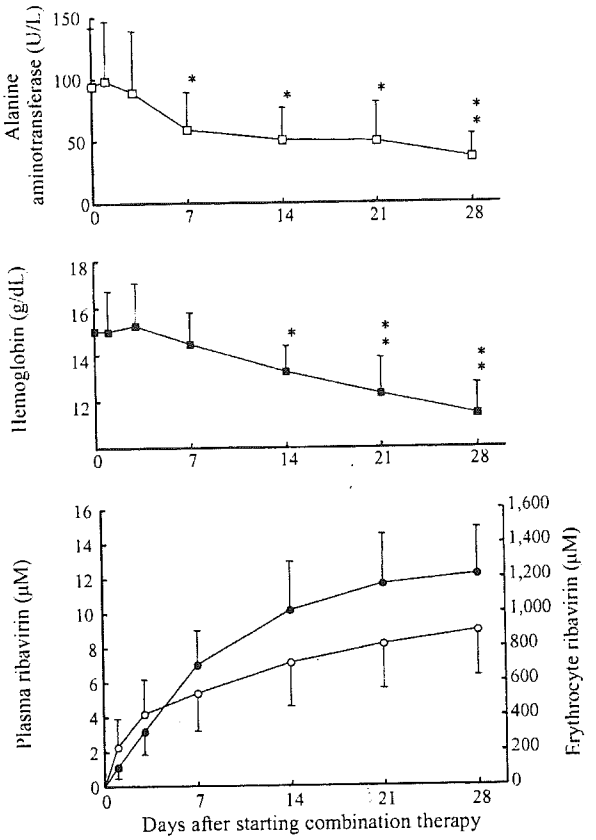

Fig. 1. Change in plasma (○) and erythrocyte (●) ribavirin concentrations, and consequent reduction of hemoglobin (■) and alanine aminotransferase (□) levels after starting interferon alpha-2b and ribavirin combination therapy. Significant differences were observed at $^{*}p < 0.05$ and $^{**}p < 0.0001$.

There was no correlation between Hb reduction and the daily dose of ribavirin (mg/kg/day) (data not shown). Significant correlation was not observed between Hb reduction and ribavirin concentration on day 14 (Fig. 2) when significant Hb reduction from baseline was firstly observed after starting the combination therapy (Fig. 1). However, weak correlation

Table 2
Ribavirin concentrations and changes in hemoglobin, hematocrit and alanine aminotransferase levels 28 days after starting combination therapy

Groups	Steady-state ribavirin concentration (μM) of	
	<1000 ($n = 7$)	≥1000 ($n = 12$)
Ribavirin dose (mg/kg/day)	12.1 ± 1.5	11.2 ± 1.4
Ribavirin concentration (μM)		
Plasma	7.5 ± 1.9	9.8 ± 2.7
Erythrocyte**	941 ± 63	1377 ± 197
Hemoglobin (g/dL)	11.8 ± 1.6	11.3 ± 1.0
ΔHemoglobin*	2.6 ± 0.9	3.8 ± 1.2
Hematocrit (%)	35 ± 5	33 ± 3
ΔHematocrit*	7 ± 4	12 ± 4
Alanine aminotransferase (U/L)	33 ± 20	38 ± 19
ΔAlanine aminotransferase	71 ± 54	43 ± 32

Data are expressed as mean ± S.D. (Δ) Difference in the values between baseline and day 28.
* Significant difference between two groups was observed at $p < 0.05$.
** Significant difference between two groups was observed at $p < 0.001$.

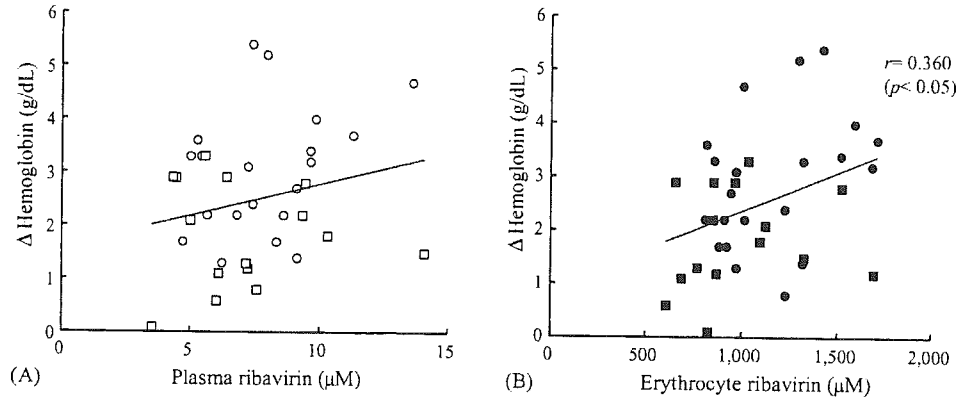

Fig. 2. Correlation between hemoglobin reduction from the baseline and plasma (A, open symbol) and erythrocyte (B, closed symbol) ribavirin concentration 14–28 days after starting the combination therapy. Square symbol and circle symbol represented data on day 14 and data from days 21 to 28, respectively. (Δ) Difference in the values from baseline.

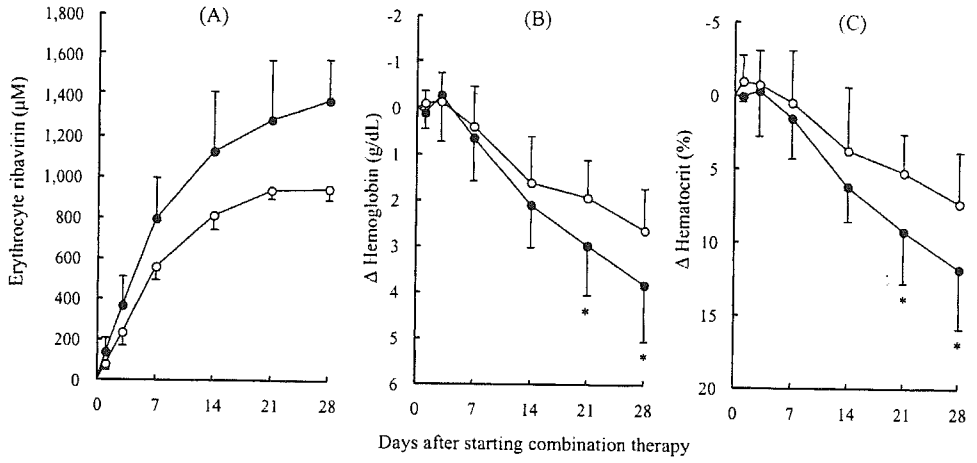

Fig. 3. Change in erythrocyte ribavirin concentrations (A), Δhemoglobin (B) and Δhematocrit (C). (Δ) Difference in the values from baseline. Closed circle (●) and open circle (○) represented higher steady-state erythrocyte ribavirin (≥1000 μM) group and lower (<1000 μM) group, respectively. Significant differences were observed between the two groups: $^{*}p < 0.05$.

was found between Hb reduction and erythrocyte ribavirin 14–28 days after starting the combination therapy ($r = 0.360$, $p < 0.05$), but not with plasma ribavirin (Fig. 2).

The patients with higher levels of erythrocyte ribavirin (≥1000 μM) at steady-state had greater Hb and Ht reduction compared with those of the patients with lower levels (<1000 μM) (Fig. 3). Significant differences in Hb and Ht reduction from the baseline were observed between the groups with higher and lower levels of erythrocyte ribavirin ($p < 0.05$) (Table 2). Nine cases out of 12 patients who developed anemia within the first 28 days of the combination therapy had higher levels of erythrocyte ribavirin (≥1000 μM). There was no significant difference in ribavirin dose and ALT reduction between the two groups (Table 2).

4. Discussion

Marked elevation of erythrocyte ribavirin concentration including its phosphorylated metabolites (149-fold versus plasma ribavirin concentration) was observed in 19 HCV patients following interferon alpha-2b and ribavirin combination therapy. Steady-state erythrocyte ribavirin concentration was 1218 ± 270 μM within 28 days after starting the combination therapy (Fig. 1; Table 1). These pharmacokinetic data were almost same with our previous study of a small number of patients [10,14]. We confirmed that erythrocyte ribavirin concentration showed significant correlation with Hb reduction (Fig. 2). Significant correlation between erythrocyte ribavirin (not plasma ribavirin) and Hb reduction ($r = 0.360$, $p < 0.05$) suggested that the erythrocyte ribavirin would be a preferable parameter for assessing ribavirin-induced hemolytic anemia. We further evaluated erythrocyte ribavirin levels over 1000 μM, which induced intracellular ATP reduction in in vitro [8]. Our finding in practical HCV treatment, which erythrocyte ribavirin levels over 1000 μM induced greater Hb reduction and developing anemia (Fig. 3; Table 2), also supports that a possible mechanism of ribavirin-induced anemia, confirmed in in vitro study [8].

Several researchers determined plasma ribavirin concentration and found the correlation between plasma ribavirin

and viral response [15–18]. Arase et al. suggested that the desirable serum ribavirin concentrations for higher sustained viral response were 12.3–14.3 μM at a steady state [15]. We support the determining plasma levels to conduct therapeutic drug monitoring of ribavirin for sufficient clinical outcome of the combination therapy. We further emphasize the importance of the determination of erythrocyte ribavirin concentration to achieve safe combination therapy in addition to the determination of plasma ribavirin. Significant correlation was not observed between Hb reduction and ribavirin dose (mg/kg/day) (data not shown). This observation was compatible with the report by Van Vlierberghe et al. [19]. Since the degree of Hb and Ht reduction might be dependent on erythrocyte ribavirin concentration and a possible threshold of the onset of Hb and Ht reduction might be around 1000 μM (Fig. 3), dose modification of oral ribavirin might be considered when the erythrocyte ribavirin concentration over 1000 μM and severe Hb reduction are observed simultaneously. Optimal dose modification leads to the enhancement of adherence to the combination therapy, resulting in higher virological response as well as avoiding severe anemia [20].

In conclusion, erythrocyte ribavirin was strongly associated with Hb reduction in interferon and ribavirin combination therapy. It was confirmed that the higher erythrocyte ribavirin concentration (≥1000 μM), in which impairing erythrocyte integrity had been observed in in vitro study for the action mechanism of ribavirin-induced anemia, produced severe Hb reduction in patients under interferon and ribavirin combination therapy.

Acknowledgments

We greatly appreciate for useful discussion with Prof. Tanaka N., Prof. Mitamura K., and Dr. Ikegami T. We also thank to Miss Wakae M. for her technical assistance.

References

[1] McHutchison JG, Gordon SC, Schiff ER, et al. Interferon alfa-2b alone or in combination with ribavirin as initial treatment for chronic hepatitis C. Hepatitis Interventional Therapy Group. N Engl J Med 1998;339:1485–92.

[2] Manns MP, McHutchison JG, Gordon SC, et al. Peginterferon alpha-1b plus ribavirin compared with interferon alpha-2b plus ribavirin for initial treatment of chronic hepatitis C: a randomised trial. Lancet 2001;358:958–65.

[3] Reichard O, Norkrands G, Fryden A, Braconier JH, Sonnerborg A, Weiland O. Randomised, double-blind, placebo-controlled trial of interferon alpha-2b with and without ribavirin for chronic hepatitis C. The Swedish Study Group. Lancet 1998;351:83–7.

[4] Shiffman ML, Di Bisceglie AM, Lindsay KL, et al. Peginterferon alpha-2a and ribavirin in patients with chronic hepatitis C who have failed prior treatment. The HALT-C trial group. Gastroenterology 2004;124:642–50.

[5] Chang CH, Chen KY, Lai MY, Chan KA. Meta-analysis: ribavirin-induced haemolytic anaemia in patients with chronic hepatitis C. Aliment Pharmacol Ther 2002;16:1623–32.

[6] Fried MW. Side effects of hepatitis C and their management. Hepatology 2002;36:S237–44.

[7] Gaeta GB, Precone DF, Felaco FM, et al. Premature discontinuation of interferon and ribavirin for adverse effects: a multicentre survey in 'real world' patients with chronic hepatitis C. Aliment Pharmacol Ther 2002;16:1633–9.

[8] De Franceschi L, Fattovich G, Turrini F, et al. Hemolytic anemia induced by ribavirin therapy in patients with chronic hepatitis C virus infection: role of membrane oxidative damage. Hepatology 2000;31:997–1004.

[9] Homma M, Jayewardene AL, Gambertoglio J, Aweeka F. High-performance liquid chromatographic determination of ribavirin in whole blood to assess disposition in erythrocytes. Antimicrob Agents Chemother 1999;43:2716–9.

[10] Inoue Y, Homma M, Matsuzaki Y, et al. Liquid chromatography assay for routine monitoring of cellular ribavirin levels in blood. Antimicrob Agents Chemother 2004;48:3813–6.

[11] Javis SM, Thorn JA, Glue P. Ribavirin uptake by human erythrocytes and the involvement of nitrobenzylthioinosine-sensitive (es) nucleoside transporters. Br J Pharmacol 1998;123:1587–92.

[12] Wu JZ, Larson G, Walker H, Shim JH, Hong Z. Phosphorylation of ribavirin and viramidine by adenosine kinase and cytosolic 5′-nucleotidase II: implications for ribavirin metabolism in erythrocytes. Antimicrob Agents Chemother 2005;49:2164–71.

[13] Lau JY, Tam RC, Liang TJ, Hong Z. Mechanism of action of ribavirin in the combination treatment of chronic HCV infection. Hepatology 2002;35:1002–9.

[14] Homma M, Matsuzaki Y, Inoue Y, et al. Marked elevation of erythrocyte ribavirin levels in interferon and ribavirin-induced anemia. Clin Gastroenterol Hepatol 2004;2:337–9.

[15] Arase Y, Ikeda K, Tsubota A, et al. Significance of serum ribavirin concentration in combination therapy of interferon and ribavirin for chronic hepatitis C. Intervirology 2005;48:138–44.

[16] Jen JF, Glue P, Gupta S, Zambas D, Hajian G. Population pharmacokinetic and pharmacodynamic analysis of ribavirin in patients with chronic hepatitis C. Ther Drug Monit 2000;22:555–65.

[17] Tsubota A, Akuta N, Suzuki F, et al. Viral dynamics and pharmacokinetics in combined interferon alfa-2b and ribavirin therapy for patients infected with hepatitis C virus of genotype 1b and high pretreatment viral load. Intervirology 2002;45:33–42.

[18] Tsubota A, Hirose Y, Izumi N, Kumada H. Pharmacokinetics of ribavirin in combined interferon-alpha-2b and ribavirin therapy for chronic hepatitis C virus infection. Br J Clin Pharmacol 2003;55:360–7.

[19] Van Vlierberghe H, Delanghe JR, De Vos M, Leroux-Roel G, BASL Steering Committee. Factors influencing ribavirin-induced hemolysis. J Hepatol 2001;34:911–6.

[20] McHutchison JG, Manns M, Patel K, et al. Adherence to combination therapy enhanced sustained response in group-1-infected patients with chronic hepatitis C. International Hepatitis Interventional Therapy Group. Gastroenterology 2002;123:1061–9.

Enhancement of DNA topoisomerase I inhibitor–induced apoptosis by ursodeoxycholic acid

Tadashi Ikegami,[1,2] Yasushi Matsuzaki,[1] Maryam Al Rashid,[4] Susan Ceryak,[2,3] Yining Zhang,[1] and Bernard Bouscarel[2,4]

[1]Division of Gastroenterology and Hepatology, Institute of Clinical Medicine, University of Tsukuba, Tsukuba City, Japan and [2]Departments of Medicine, [3]Pharmacology and Physiology, and [4]Biochemistry and Molecular Biology, George Washington University Medical Center, Washington, District of Columbia

Abstract

Certain hydrophobic bile acids, including deoxycholic acid and chenodeoxycholic acid, exert toxic effects not only in the liver but also in the intestine. Moreover, ursodeoxycholic acid (UDCA), which has protective actions against apoptosis in the liver, may have both protective and toxic effects in the intestine. The goal of the present study was to clarify the mechanisms responsible for the toxic effect of UDCA in intestinal HT-29 cells. Here, we show that UDCA potentiated both phosphatidylserine externalization and internucleosomal DNA fragmentation induced by SN-38, the most potent metabolite of the DNA topoisomerase I inhibitor, CPT-11. Furthermore, the loss of mitochondrial membrane potential as well as mitochondrial membrane permeability transition induced by SN-38 was enhanced in the presence of UDCA, resulting in an increased lethality determined by colony-forming assay. This UDCA-induced increased apoptosis was not due to alteration of either intracellular accumulation of SN-38 or cell cycle arrest by SN-38. The increased apoptosis was best observed when UDCA was present after SN-38 stimulation and was independent of caspase-8 but dependent on caspase-9 and caspase-3 activation. Furthermore, UDCA enhanced SN-38-induced c-Jun NH_2-terminal kinase activation. In conclusion, UDCA increases the apoptotic effects while decreasing the necrotic effects of SN-38 when added after the topoisomerase I inhibitor, showing potential clinical relevance as far as targeted cell death and improved wound healing are concerned. However, the use of this bile acid as an enhancer in antitumor chemotherapy should be further evaluated clinically. [Mol Cancer Ther 2006;5(1):68–79]

Introduction

CPT-11 [7-ethyl-10-4-(1-piperidino)-1-piperidinocarbonyloxycamptothecin] has been approved worldwide for the treatment of colorectal cancer and is under extensive investigation and therapeutic evaluation for a variety of other cancers (1–4). Both CPT-11 and SN-38, its 7-ethyl-10-hydroxycamptothecin derivative from carboxylesterase-induced hydrolysis (5), present antitumor activity through the inhibition of DNA topoisomerase I (6). SN-38 has at least a 1,000-fold more potent antitumor effect than CPT-11 as shown *in vitro* (6). CPT-11 and SN-38 stabilize the topoisomerase I-DNA complex, and its collision with the DNA replication fork leads to the generation of permanent strand breaks and to cell death (7). Stabilization of the cleavable complexes by CPT-11/SN-38 is accompanied by a G_2-M arrest and apoptosis (8, 9). Although the mechanism is still unclear, the apoptotic effect of CPT-11 associated with an increased DNA fragmentation has been reported previously in a variety of colon cancer cell lines (8). The apoptotic effect of CPT-11 in colon carcinoma and/or lung cancer cells has been linked not only with an increased cleavage of poly(ADP-ribose) polymerase, characteristic of programmed cell death, but also with an alteration of proapoptotic and antiapoptotic proteins, including Bax, Bcl-x_L, and Bcl-2 (8, 10). Furthermore, these apoptotic effects of the camptothecin derivatives are at least p53 dependent (see ref. 11 for review).

Bile acids are believed to play an important role in the etiology of colorectal cancer, which is one of the leading causes of cancer-related deaths in the world (12). Several studies consider hydrophobic secondary bile acids, such as deoxycholic acid, to be tumor promoters and to exert their cytotoxicity through apoptosis (13, 14). One of the possible apoptotic effects of bile acids is attributed to the perturbation of mitochondrial functions (15, 16). As a result of damage and loss of transmembrane potential, the mitochondria either release cytochrome *c* or Smac/DIABLO into the cytosol. The former, in turn, binds to Apaf-1 and induces caspase-9-dependent activation of caspase-3, whereas the latter blocks the inhibitory effects of inhibitor of apoptosis proteins on caspases (17, 18). Both pathways promote cell death.

Not all bile acids have cytotoxic properties. The dihydroxy bile acid, ursodeoxycholic acid (UDCA), has

Received 4/6/05; revised 10/14/05; accepted 10/28/05.

Grant support: Daiichi Pharmaceutical Co. Ltd., Yakult Honsha Co. Ltd., and Mitsubishi Welpharma Co. Ltd. and NIH grant R01 DK56108 (B. Bouscarel).

The costs of publication of this article were defrayed in part by the payment of page charges. This article must therefore be hereby marked advertisement in accordance with 18 U.S.C. Section 1734 solely to indicate this fact.

Note: Presented in part at the Annual Meeting of the American Gastroenterological Association in May 2001 and Annual Meeting of the AACR in July 2003.

Requests for reprints: Bernard Bouscarel, George Washington University Medical Center, 2300 Eye Street, Northwest Ross Hall, Room 523, Washington, DC 20037. Phone: 202-994-2114; Fax: 202-994-3435. E-mail: bbouscarel@mfa.gwu.edu

doi:10.1158/1535-7163.MCT-05-0107

been shown to exert antiapoptotic effects (15). Although the antiapoptotic mechanism of UDCA is still under discussion, several reports have hypothesized this bile acid to stabilize the mitochondrial structure (15). However, this bile acid may also have proapoptotic actions: (*a*) UDCA potentiated photodamage in leukemia cells (19), (*b*) UDCA did not protect against apoptosis induced by hydrophobic bile acids in several colonic cancer cell lines (20), and (*c*) UDCA induced apoptosis in hepatocytes when both mitogen-activated protein kinase (MAPK) and phosphatidylinositol 3-kinase pathways were inhibited (21). Therefore, UDCA may act differentially on death and survival pathways depending on the cell type, physiologic conditions, and/or stimulus. Thus, the clarification of the mechanism of UDCA action especially in terms of antiapoptotic or proapoptotic effects is relevant to foster a better understanding and to widen the clinical usage of this bile acid. The hypothesis that UDCA potentiates the SN-38-induced cytotoxicity, which in turn could increase the chemotherapeutic effect of this camptothecin derivative, is attractive. Indeed, a recent report indicated that coadministration of UDCA with photodynamic therapy resulted in augmented antitumor effects (19).

The aim of the present study was to investigate the mechanism of action of UDCA on the series of events associated with cell death, such as cell cycle alteration, apoptosis, and growth inhibition induced by SN-38. The possible involvement of mitochondrial membrane potential ($\Delta\Psi_m$) and caspases in the action of UDCA was also examined. An attempt was made to delineate key protein kinases activated by this bile acid. The colon-derived adenocarcinoma HT-29 cell line, a representative colon cancer cell line, was used as the predominant model for these studies. However, the colonic adenocarcinoma LS174T and Caco-2 and the hepatic HepG2 cells were used for comparison.

Materials and Methods

Materials

SN-38 and radiolabeled SN-38 ([^{14}C]SN-38) were kindly supplied by Yakult Honsha Co. Ltd. (Tokyo, Japan) and were 98% to 99% pure as judged by gas-liquid chromatography. UDCA, tauroursodeoxycholic acid, chenodeoxycholic acid, and taurocholic acid were kindly supplied by Mitsubishi Welpharma Co. Ltd. (Osaka, Japan). Green fluorescent protein (GFP)–labeled Annexin V was obtained from Clontech (Palo Alto, CA). Propidium iodide (PI) was obtained from Sigma Chemical Co. (St. Louis, MO). Tetramethylrhodamine, xanthylium, 3,6-bis(dimethylamino)-9-[2-(methoxycarbonyl) phenyl], perchlorate (TMRM; Mitotracker-1) and 5,5′,6,6′-tetrachloro-1,1′,3,3′-tetraethylbenzimidazolylcarbocyanine iodide (JC-1) were obtained from Molecular Probes (Eugene, OR). The specific caspase inhibitors (z-DEVD-fmk, z-IETD-fmk, z-LEHD-fmk, and Z-VAD-fmk) were obtained from Trevigen, Inc. (Gaithersburg, MD). PD98059 and SP600125 were obtained from Calbiochem (San Diego, CA). The human colon adenocarcinoma cell line HT-29 was from the American Type Culture Collection (Manassas, VA). DMEM was from Life Technologies, Inc. (Frederick, MD).

Cell Culture and Clonogenic Assay

HT-29 cells were grown in DMEM containing 10% fetal bovine serum, 50 units/mL penicillin G, and 50 μg/mL streptomycin at pH 7.4 and maintained at 37°C in a humidified atmosphere of 5% CO_2. Clonogenic lethality of SN-38 and UDCA was determined as described previously (9). In brief, the HT-29 cells were treated with increasing concentrations of SN-38 for 2 hours. After removal of the drug by washing twice with PBS, the cells were further incubated for 24 hours in the presence or absence of UDCA. Cells (n = 500) were reseeded in triplicate in 60-mm culture dishes containing 3 mL DMEM. The colonies were grown for 2 weeks, washed with PBS, fixed with 80% methanol, stained with methylene blue (0.04%), and counted using an Eagle Eye II transilluminator (Stratagene, La Jolla, CA). During colony growth, the culture medium was replaced every 3 days. Cloning efficiency for untreated HT-29 cells was ~74%.

Semiquantification of DNA Fragmentation

The comet assay or single-cell gel electrophoresis assay is based on the alkaline lysis of labile DNA at sites of damage. The unwound, relaxed DNA is able to migrate out of the cell during electrophoresis and can be visualized by SYBR Green (Molecular Probes) staining. Cells that have accumulated DNA damage appear as fluorescent comets with tails of DNA fragmentation or unwinding, whereas normal undamaged DNA does not migrate far from the origin. The fluorescence intensity of these cells was determined by using an ACAS570 laser scanner cytometer (Meridian Instruments, Inc., Okemos, MI). The tail length and the head were selected for the quantification of DNA migration, and the ratio of these values was calculated.

Annexin V and PI Staining

The apoptotic HT-29 cells were determined by using GFP-labeled Annexin V and in accordance with the manufacturer's instructions as described previously (9). Binding affinity for GFP-Annexin V and PI was determined by flow cytometric analysis (FACScan, Becton Dickinson, San Jose, CA). Excitation wavelength was 488 nm, and the emission wavelengths were 530 nm (FL1) for GFP and 620 nm (FL2) for PI. Fluorescence cutoff for the FL1 and FL2 channel was defined using HT-29 cells permeabilized with 0.1% Triton X-100–containing PBS.

Effect of SN-38 and UDCA on mRNA Expression Level of Key Proteins Regulating Cell Cycle and Apoptosis

mRNA expression level was quantitated by RNase protection assay with a ^{32}P-labeled multitranscript probe containing gene sequences for the antiapoptotic proteins Bcl-W, Bcl-x_L, and Bcl-2, the proapoptotic proteins Bcl-x_S and Bax, and the cyclin-dependent kinase inhibitors, $p21^{waf1/cip}$, $p15^{INK4B}$, and $p16^{INK4A}$ according to the manufacturer's instructions (BD PharMingen, San Diego, CA). Protected ^{32}P-labeled probes were resolved on a 5% acrylamide sequencing gel, and the dried gel was exposed

to a phosphor screen (Amersham, Piscataway, NJ). Relative expression was determined by densitometric analysis, using a Molecular Dynamics STORM PhosphorImager (Piscataway, NJ) and ImageQuant software, and normalized to the respective expression of two housekeeping genes, *L32* and *glyceraldehyde-3-phosphate dehydrogenase*. Finally, the normalized results were expressed as percentage of the respective control.

Determination of $\Delta\Psi_m$

HT-29 cells were incubated with 1 μg/mL of the $\Delta\Psi_m$-sensitive dye, JC-1, for 30 minutes at 37°C, gently harvested with trypsin, washed in PBS, resuspended in medium at a density of ~ 1×10^7/mL, and transferred on ice to the flow cytometer. JC-1 was excited at 488 nm and the monomer signal (green) was analyzed at 525 nm (FL1) on a flow cytometer using a minimum of 10,000 cells per sample. Simultaneously, the aggregate signal (red) was analyzed at 590 nm (FL2). FCCP (1 μmol/L, Sigma), a known mitochondrial inhibitor, was used as positive control for mitochondrial depolarization. The ratio of the signal at 590 nm to the signal at 525 nm was determined after background subtraction and expressed as percentage of control.

Confocal Laser Scanning Microscopy

To visualize the mitochondria permeability transition, the HT-29 cells were stained with TMRM and acetoxymethylester of calcein (calcein-AM, Wako Chemicals, Tokyo, Japan) and observed by confocal laser scanning microscopy (Leica TCS SP2, Leica Microsystems AG, Wetzlar, Germany) as reported previously by Nieminen et al. (22). In brief, HT-29 cells were loaded in culture medium with 500 nmol/L TMRM and 1 μmol/L calcein-AM for 20 minutes at 37°C, washed with PBS, and mounted on the microscope stage. Under this condition, calcein-AM accumulated virtually exclusively in the cytosol, and mitochondria were imaged as voids in the cytosolic fluorescence. Onset of permeability of mitochondrial membranes to calcein-AM was indicated by filling of mitochondrial voids.

Topoisomerase I, c-Jun NH_2-Terminal Kinase, and Extracellular Signal-Regulated Kinase Expression Levels and Caspase Activity Determination

Total cellular proteins (10–20 mg/mL) were separated by SDS-PAGE according to the method of Laemmli (23) and transferred to polyvinylidene difluoride membranes. Blots were probed with specific antibodies to the respective β-actin and topoisomerase I (Santa Cruz Biotechnology, Santa Cruz, CA), phosphorylated and total c-Jun NH_2-terminal kinase (JNK), and extracellular signal-regulated kinase (ERK; Cell Signaling, Beverly, MA) followed by the appropriate secondary horseradish peroxidase–labeled antibody. The immunoreactive proteins were visualized by enhanced chemiluminescence, analyzed by densitometric scanning, and normalized to the respective β-actin or total kinase absorbance signals.

The specific caspase activity in HT-29 cell lysates was determined using a caspase colorimetric activity assay kit (Chemicon International, Temecula, CA) according to the manufacturer's instruction.

Statistical Analysis

Except as otherwise indicated, results were expressed as mean ± SE. The statistical significance of the means was determined by either one-way ANOVA or Student's *t* test.

Results

UDCA Enhanced the Lethality of SN-38-Treated HT-29 Cells

Exposure of HT-29 cells to 50 μmol/L UDCA alone for 24 hours had no effect on colony-forming ability (data not shown). The colony-forming ability of the cells treated with 0.5 μmol/L SN-38 for 2 hours was significantly ($P < 0.001$) inhibited by ~ 50% when compared with control (Fig. 1A). After removal of SN-38, the addition of 2.5 to 10 μmol/L UDCA was without effect; however, the addition of 50 μmol/L UDCA for 24 hours resulted in a significant ($P < 0.01$) further reduction in colony formation by 20% to 25% when compared with that of the cells treated with SN-38 alone, supporting an UDCA-induced enhancement of SN-38 clonogenic lethality. Furthermore, SN-38 concentrations

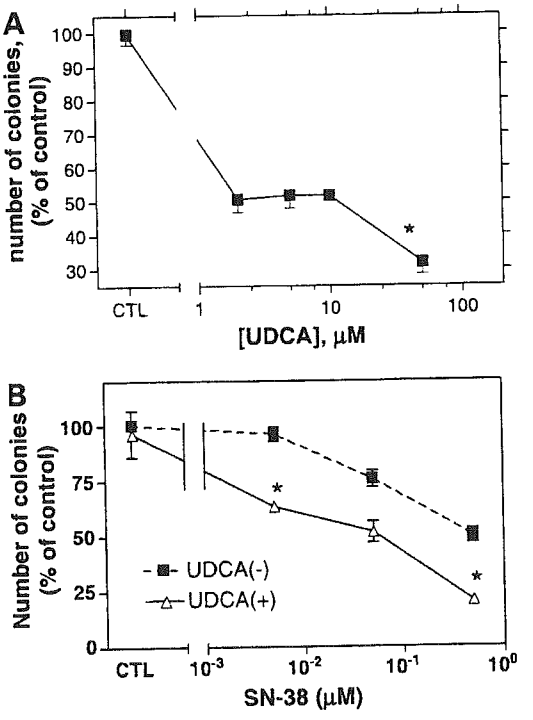

Figure 1. Growth inhibition of HT-29 cells and topoisomerase I protein expression induced by SN-38 and UDCA. **A**, HT-29 cells were incubated for 2 h with 0.5 μmol/L SN-38. After removal of SN-38, the cells were further incubated with increasing concentrations of 2.5 to 50 μmol/L UDCA for 24 h, collected by trypsinization, and then seeded in fresh culture dishes (500 per dish). Colonies grown after 2 wks were counted and expressed as percentage of control (*CTL*). **B**, HT-29 cells were incubated for 2 h with increasing concentrations (0.005 – 0.5 μmol/L) of SN-38, and after removal, the cells were further incubated with 50 μmol/L UDCA for 24 h and processed as described above. *Points*, mean of three independent experiments; *bars*, SE. *, $P < 0.01$, significantly different from SN-38 treatment without UDCA.

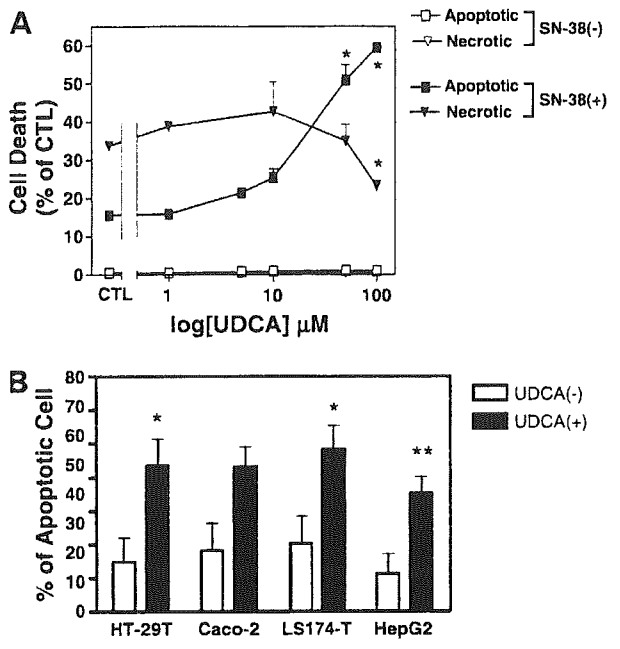

Figure 2. SN-38-induced phosphatidylserine externalization is enhanced by UDCA. **A**, HT-29 cells were incubated in the presence and absence of 0.5 μmol/L SN-38 for 2 h. After replacement of the culture medium, the cells were further incubated with increasing concentrations (1–100 μmol/L) of UDCA for 48 h. Percentage of apoptotic and necrotic cells was determined by flow cytometry using both GFP-Annexin V and PI. The GFP only–positive cells were defined as apoptotic, whereas GFP– and PI-positive cells were defined as necrotic. *Points*, mean percentage of control from two independent experiments done in duplicate; *bars*, SE. *, $P < 0.001$, significantly different from control. **B**, under the same conditions, HT-29, LS174T, Caco-2, and HepG2 cells were incubated in parallel with 1 μmol/L SN-38 in the presence (+) or absence (-) of 100 μmol/L UDCA for 72 h. Apoptotic cells were determined by Annexin V/PI binding assay. *, $P < 0.01$; **, $P < 0.05$.

≥0.05 μmol/L significantly increased clonogenic lethality by 20% to 50%, whereas in the presence of 50 μmol/L UDCA a SN-38-induced clonogenic lethality of 30% was observed at a concentration as low as 0.005 μmol/L (Fig. 1B). Moreover, although still under investigation, the UDCA-induced increase in SN-38 lethality was apparently independent of an alteration in topoisomerase I protein expression level (data not shown).

Effect of UDCA on SN-38-Induced Cell Death

We have reported previously that 35% of the cells treated with 0.5 to 1 μmol/L SN-38 had externalized phosphatidylserine on the plasma membrane, one of the early-phase phenomena of apoptotic cell death (9). Thus, we studied whether the magnitude of the phosphatidylserine externalization induced by SN-38 was altered by UDCA. In this assay, both Annexin V– and PI-positive cells were considered to be necrotic as described previously (9). For these studies, both floating and attached cells were collected and subjected to FACS analysis. As shown in Fig. 2A, 0.5 μmol/L SN-38 alone induced phosphatidylserine externalization in 16 ± 4.3% of the cells after the 48-hour incubation period. Under these conditions, the percentage of necrotic cells (Annexin V– and PI-positive) was 33.2 ± 4.6%. The addition of UDCA after initial SN-38 exposure presented a dose-dependent increase in Annexin V–positive cells (early apoptosis). This increase reached ~60% in the presence of 100 μmol/L UDCA and was significantly different from control ($P < 0.001$). Concurrently, the percentage of Annexin V/PI–positive cells (primary and secondary necrosis) was significantly decreased in a dose-dependent manner to 23.4 ± 1.2% with 100 μmol/L UDCA. However, UDCA alone had no significant effect on phosphatidylserine externalization at the various concentrations tested. Furthermore, although not shown, the majority of the Annexin V–positive cells were among the floating rather than attached cells. This suggests that, in our system, the cell detachment occurred at an early phase in SN-38-induced HT-29 cell death. To determine whether this effect was cell specific, we did similar studies using colonic adenocarcinoma Caco-2 and LS174T cells as well as the hepatocarcinoma HepG2 cell line. The cells were incubated with 1 μmol/L SN-38 for 2 hours and, after washing, for an additional 72 hours without or with 100 μmol/L UDCA. Apoptosis was determined as described above. The results in Fig. 2B indicate that the significantly increased apoptotic effect of UDCA in the presence of SN-38 was not specific to HT-29 cells and was also observed in certain other colonic (LS174T) and hepatic (HepG2) cell lines. However, although the tendency remained, the effect of UDCA on Caco-2 cells was not significant.

Optimal Incubation Period for the Proapoptotic Action of UDCA

Preincubation with UDCA is prerequisite for its proapoptotic action on a photoirradiated cancer cell line (19). Therefore, to clarify the critical period of incubation of the cells with UDCA to induce optimum SN-38 toxicity, the HT-29 cells were incubated with 100 μmol/L UDCA either 24 hours before SN-38 exposure (pre-UDCA), during the 2-hour SN-38 exposure (co-UDCA), or after SN-38 exposure (post-UDCA) and for an additional 72 hours (Fig. 3A). In addition, in a subsequent experiment, UDCA was added after SN-38 removal and for either 72 hours or the last 48 and 24 hours of the experiment (Fig. 3B). The phosphatidylserine externalization was then quantified as indicated in Materials and Methods. Although UDCA addition had no effect when added before or during SN-38 exposure (Fig. 3A), it increased SN-38-induced apoptosis by >100% when added after removal of SN-38. The increased UDCA effect was significant after a period as short as 24 hours (30%) and was a function of the period of incubation with this bile acid (Fig. 3B).

Apoptotic Action of SN-38 and UDCA Detected by DNA Fragmentation

DNA fragmentation represents a hallmark of apoptosis regardless of whether the apoptotic process has been initiated by either intrinsic signals or death receptors involving extrinsic signals. Two major steps have been identified in the apoptosis-associated DNA fragmentation. The first step involves formation of high molecular weight DNA fragments of 50 to 300 kb. The second step generates

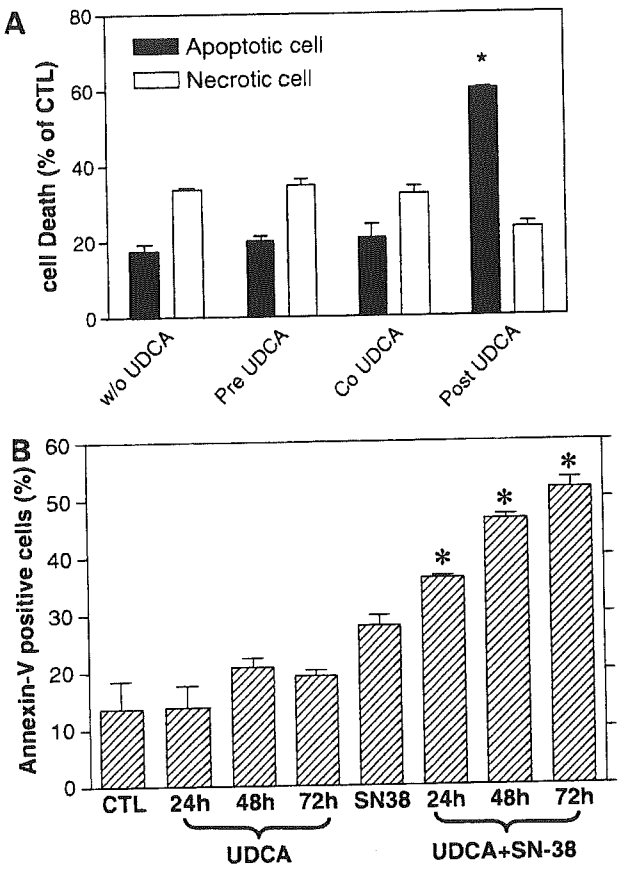

Figure 3. Effect of the period of incubation of UDCA on SN-38-induced apoptosis. **A**, HT-29 cells were incubated with 0.5 μmol/L SN-38 for 2 h and in the absence (*w/o UDCA*) and presence of 100 μmol/L UDCA for various periods. *Pre UDCA*, cells were incubated with UDCA for 24 h, removed, and then incubated with SN-38 for 2 h; *Co UDCA*, cells were incubated with SN-38 and UDCA simultaneously for 2 h; *Post UDCA*, after 2-h incubation with SN-38, cells were further incubated with UDCA for 72 h. *, $P < 0.01$, significantly different compared with w/o UDCA. **B**, cells were incubated in the absence (*CTL*) or presence of SN-38 for 2 h and then washed with PBS and further incubated with UDCA (100 μmol/L) for the last either 24, 48, or 72 h. Percentage of apoptotic and/or necrotic cells at the end of the incubation period was determined by flow cytometric analysis using Annexin V/PI. *, $P < 0.05$, significantly different from SN-38 alone.

small, 200- to 300-bp DNA fragments. These small fragments lead to DNA ladder formation classically associated with apoptosis. Initially, we determined the effect of UDCA on SN-38-induced DNA fragmentation by using DNA electrophoresis. UDCA alone has no effect on DNA fragmentation. However, the electrophoresis of the small molecular weight DNA revealed that 0.5 to 2 μmol/L SN-38 alone induced DNA fragmentation in a dose-dependent fashion (Fig. 4A). Furthermore, the addition of 50 μmol/L UDCA after removal of SN-38 and for 72 hours enhanced this DNA ladder formation induced by SN-38 at every concentration tested.

For quantification purposes and to support these above observations, single-cell electrophoresis (i.e., comet assay) was used. In this assay, fragmented DNA can migrate through permeabilized nuclear membranes as well as plasma membranes, producing a "tail" from the nuclear head. The overall shape resembles that of a comet. Either control cells or 100 μmol/L UDCA-treated cells did not induce any significant DNA tail formation (Fig. 4B and C). SN-38 treatment induced the formation of a tail suggesting DNA fragmentation in these cells, mimicking the smear pattern observed in conventional agarose gel electrophoresis (Fig. 4A). Furthermore, the addition of UDCA resulted in the extension of the tail induced by SN-38 alone, which represents greater DNA fragmentation (Fig. 4B). The calculated ratio of the fluorescence intensity of the tail to head increased in a time-dependent fashion by SN-38 (Fig. 4C). Although the tail formation in the cells treated with SN-38 alone was not significantly different from control, the addition of 100 μmol/L UDCA for 24 hours induced a significant ~3-fold increase ($P < 0.01$). At 48 hours, SN-38 induced a 15.2-fold increase in tail formation compared with control ($P < 0.01$), and the addition of 100 μmol/L UDCA further enhanced the tail formation by ~1.6-fold ($P < 0.05$), suggesting the facilitation of apoptotic cell death by UDCA. Taken together, these results support the enhancement of SN-38 lethality by UDCA to be due to the augmentation of apoptotic cell death.

Effect of UDCA on HT-29 Cellular Uptake and Efflux of SN-38 and on Cell Cycle

The intracellular accumulation of SN-38 in the presence of UDCA was determined to assess any possible alteration in the HT-29 cellular uptake or efflux of SN-38 by the bile acid. After 2-hour incubation, SN-38 was removed and the cells were further incubated with 100 μmol/L UDCA. The intracellular accumulation of SN-38 in HT-29 cells was measured with [^{14}C]SN-38. The intracellular concentrations following 2- and 24-hour incubation of the cells with 0.5 μmol/L SN-38 were 70 ± 11 and 59 ± 4 pmol/10^6 cells and were not significantly different (68 ± 7 and 70 ± 5 pmol/10^6 cells) when determined in the presence of 100 μmol/L UDCA. Under the same conditions, the intracellular concentrations following 2- and 24-hour incubation of the cells with 1 μmol/L SN-38 were 109 ± 5 and 158 ± 32 pmol/10^6 cells and again were not significantly different (123 ± 32 and 144 ± 18 pmol/10^6 cells) when tested in the presence of 100 μmol/L UDCA. These results are the mean ± SE of four to six different experiments.

Furthermore, SN-38 was shown to alter the HT-29 cell cycle characterized by a dose-dependent decrease in the percentage of cells in G_0-G_1 phase, a parallel increase of the cells in S phase, and an increase of those in G_2-M phase. A marked cell cycle arrest in S phase was observed with concentrations of SN-38 as low as 0.1 μmol/L but was not affected by the presence of 100 μmol/L UDCA for 24 hours (data not shown).

Effect of SN-38 and UDCA on the mRNA Expression Level of Proteins Associated to the Regulation of Both Apoptosis and Cell Cycle

One of the mechanisms of action of drug-induced cell death includes modulation of the expression of proteins